J. Physiol. (1977), **269**, *pp.* 221–254
With 2 plates and 11 text-figures
Printed in Great Britain

DEVELOPMENT OF NEUROMUSCULAR TRANSMISSION IN A LARVAL TUNICATE

BY HARUNORI OHMORI AND SHIGETO SASAKI*

From the Department of Neurophysiology, Institute of Brain Research, School of Medicine, University of Tokyo, Tokyo, Japan

(*Received 1 June 1976*)

SUMMARY

1. The time sequence of the development of acetylcholinesterase (AChE), acetylcholine (ACh) receptors and functional synapses on the embryonic muscle membrane in a tunicate larva (*Halocynthia roretzi*) was investigated *in vivo*.

2. The fertilized tunicate egg was incubated in natural sea water at 9° C. Sixty-eight hr after fertilization the free-swimming larva was hatched, which had six striated muscle fibres in the tail. The developmental stage of the embryo was indicated by the developmental hours after fertilization.

3. The transmitter at the neuromuscular junction in the hatched larva is ACh. (i) Neuromuscular transmission was completely blocked by D-tubocurarine ($1-5\times10^{-5}$ M). (ii) Eserine ($5-10\times10^{-7}$ M) approximately doubled the time constant of the falling phase of miniature excitatory junctional currents (e.j.c.s). (iii) The reversal potential of the membrane response to iontophoretically applied ACh was -10 mV and similar to that of e.j.c.s. (iv) AChE was present on the muscle membrane surface.

4. AChE activity became visible histochemically on the embryonic cell membrane in the presumptive muscle region as early as the late gastrula stage (27 hr after fertilization, 12 hr before the ACh response appeared).

5. The response to iontophoretically applied ACh was present at 39 hr after fertilization but could not be evoked at 38 hr.

6. Between 39 and 41 hr after fertilization, the ACh responses increased rapidly, then remained relatively unchanged until larval hatching.

7. The stage of the initial appearance of the ACh response corresponded to the stage when the Ca current abruptly increased in the muscle membrane.

* Present address: Laboratory of Physiology, Institute of Basic Medical Science, University of Tsukuba, Niihari-gun, Ibaraki-ken, Japan.

8. The first sign of neuromuscular transmission was appearance of a giant excitatory junctional potential (e.j.p.) with uniform amplitude (about 15–20 mV) and slow time course (time constant of the falling phase of a giant e.j.c. was $23{\cdot}4 \pm 6{\cdot}9$ msec, mean and S.D., at -60 mV and 11° C).

9. Within a few hours, these giant e.j.p.s disappeared and were successively replaced by medium-sized e.j.p.s and then e.j.p.s similar to those seen in hatched larvae (time constant of the falling phase of a miniature e.j.c. was $8{\cdot}5 \pm 1{\cdot}8$ msec at -60 mV and 11° C).

INTRODUCTION

With respect to the development of cholinergic transmission in the end-plate, it has been postulated that the ACh receptor itself is an inducer of synapse formation which then triggers the production of AChE (Sytkowsky, Vogel & Nirenberg, 1973). In order to know the causal relationships during differentiation of the chemosensitive membrane, it is important to determine *in vivo* the time sequence of the production of transmitter synthesizing or destroying enzymes, the appearance of transmitter receptors, and the formation of synapses.

The larval muscle of the tunicate is a suitable material for such studies. The developmental time from the fertilized egg to the hatched tadpole larva is only 68 hr at 9° C. The development is fairly synchronous and the hatching time is within a few hours difference if the eggs are fertilized at the same time. Only a small number of cells are included in an embryo and only six striated muscle fibres are present in the larval tail (Pl. 1*H*). The presumptive muscle cells or regions are determined already at the one cell stage, as described by Conklin's cell lineage study (1905*a*, *b*) and the large muscle cells can be easily recognized at any stage of development. The intact embryo, therefore, has the advantages of a simple system such as cultured muscle cells.

The tunicate larva has AChE which is localized only in the muscle and appears early in embryonic development (neurula stage; Durante, 1956). This suggests that the neuromuscular junction in the tunicate larva is cholinergic. Furthermore, in the tunicate embryo, the development of electrical excitability has been analysed *in vivo* during the whole ontogenic process from the unfertilized egg to the differentiated striated muscle in the larva (Takahashi, Miyazaki & Kidokoro, 1971). The aim of this study is to determine the time sequence of the development of AChE, ACh receptors and the functional synapses, i.e. the appearance of miniature e.j.p.s, in association with the development of electrical excitability in embryonic muscle membrane.

METHODS

Materials. The embryo of the tunicate, *Halocynthia roretzi*, was used. Tunicates which had eggs were kept in cold sea water aquaria at about 3° C. Whenever fresh embryos were required, the animal was transferred to a warm sea water aquarium at 11° C and raised for a few days. This procedure made the animal spawn eggs and sperm. The spawned eggs were fertilized spontaneously and they were incubated in a bath at a constant temperature of 8·5–9° C. The total period of embryonic development was about 68 h at 9° C. Since the development was fairly synchronous, the time after fertilization could be used as an indicator of the developmental stage.

TABLE 1. Development of the *Halocynthia roretzi* embryo at 9° C

Embryonic stage	Hour	Embryonic stage	Hour
2 cell	2	Late gastrula	20
4 cell	4	Neural plate	23
8 cell	6	Neurula	25
16 cell	7	Tailbud	32
32 cell	9	Melanin pigment and otolith	52
Early gastrula	16	Swimming larva	68

The relationship between morphological embryonic stage and developmenta time (hr) after fertilization. The morphological stage of the embryo could be determined within an error of 1 hr.

The morphological stage of the development was determined precisely by taking photographs every hour. The correspondence between the developmental time and the morphological stage is tabulated in Table 1. Several stages of development are illustrated in Pl. 1. Pl. 1*A* shows the gastrula stage just before closure of the blastopore. After closure of the blastopore, the neural plate is formed and the neural groove appears (Pl. 1*B*). As development advances, the embryo grows in an anterior–posterior axis and the tail appears (Pl. 1*C*). In Pl. 1*D*, the neural plate is completely covered with a layer of epithelium. At this time, the fundamental alignment of the cells in the tail region has been completed. As the tail further elongates, individual notochordal cells become clearly visible (Pl. 1*E*). When the tip of the tail touches the head within the egg shell a sphere of 0·5 mm, the head which has been smooth and round becomes elongated and its most anterior part shows an adhesive apparatus. By this time, the eye and otolith have differentiated morphologically (Pl. 1*F*). After such differentiation of the head region, the tadpole hatches and swims actively (Pl. 1*G*).

Since tunicate eggs are of a mosaic type, the presumptive regions of the muscle, the notochord, and the neurones are determined already at the one cell stage. At about the 64 cell stage, the different cell types segregate from each other (Conklin, 1905*a*, *b*). Presumptive muscle cells are aligned in two rows located on each side of the blastopore of the gastrula. After the tailbud stage, muscle cells are aligned in three rows on both sides of the notochord (Pl. 1*H*).

Electrical recording. Tunicate embryos were placed in a Lucite chamber with 15 ml. bathing solution. The follicular envelope was stripped off using fine needles under a binocular microscope. The tunica of the unhatched larva was removed by bathing in a Cellulase (Tokyo Kasei Co.) solution (2–3 ml., 10 mg/ml.) for 5–15 min. To improve penetration of muscle cells by widening the intercellular space in the epithelium, Trypsin (Tokyo Kasei Co.) solution (0·2–0·3 ml., 10,000 u./ml.) was added to

the bath and the larva was incubated for 10–20 min at 10–15° C. The muscle membrane did not seem to deteriorate by these procedures.

Two micro-electrodes (filled with 3 M-KCl and with resistances of 10–20 MΩ) were inserted by using transient current injection (Miyazaki, Takahashi & Tsuda, 1974). The membrane potential between an intracellular electrode and a 3 M-KCl agar-filled reference electrode in the bath solution was recorded with FET-input preamplifiers. For voltage clamp recording, one electrode was used for current injection. The voltage clamp circuit was the same as described in a previous paper (Okamoto, Takahashi & Yoshii, 1976). In each experiment there was no difference between the resting potential measured by the potential and current electrodes.

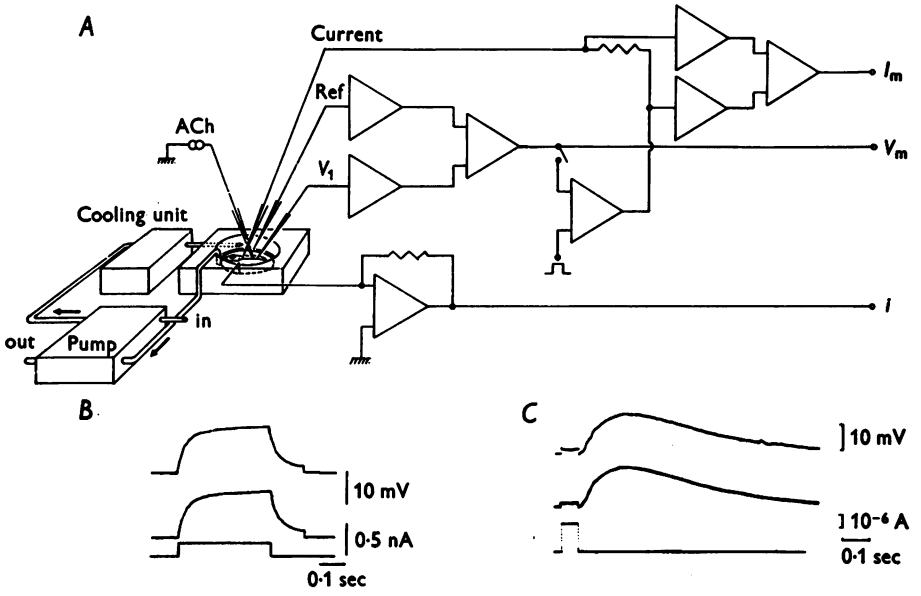

Text-fig. 1. *A*, diagram of experimental arrangement. V_m; membrane potential I_m; membrane current. i: the current iontophoretically injecting ACh. *B*, depolarizing potential responses of muscle membrane to a rectangular current pulse. The potential was recorded simultaneously by inserting two micro-electrodes separated by 500 μm into the muscle cells. *C*, the potential responses to iontophoretically applied ACh. Recording methods are the same as in *B*.

Muscle cells in the tadpole larva lie in three rows on each side of the notochord. A row is composed of seven to eight cells in series. The muscle cells on one side seemed to be connected electrotonically with each other since the recorded potentials were always similar within the group of cells on that side. The space constant along the anterior–posterior axis in the tail of the tadpole larva was measured by recording responses simultaneously from two electrodes (V_1 and V_2) separated by 200–500 μm (Text-fig. 1*B*, *C*). V_1 and V_2 showed the same potential and the same response time course to rectangular injected current pulses or iontophoretically applied ACh, indicating that the space constant at the resting potential level was long compared to the length of the tail, which was not more than 1·5 mm. Therefore, the group of

muscle cells seemed to obey the space-clamped condition at least around the resting potential.

The ACh sensitivity of muscle cells was measured by iontophoretic application of ACh (Nastuk, 1953; del Castillo & Katz, 1955). Applied current was measured by a current–voltage converter made from an operational amplifier (Text-fig. 1*A*, *i*). ACh pipettes contained 3 M ACh chloride and had a resistance of 7–10 MΩ. Iontophoretic current pulses were 10^{-7} to 8×10^{-6} A and 0·5–400 msec long. A braking current 1 to 2×10^{-7} A was applied to prevent loss of ACh from the tip of the micropipette. ACh sensitive areas were determined by positioning the ACh pipette along the muscle fibre until a maximum response and minimum latency were found. Although muscle cells are covered with a monolayer of epithelium, fairly precise localization of ACh sensitive spots was possible; they were usually around the midportion of the tail (see Text-fig. 5*C*).

The composition of standard artificial sea water (std ASW) was as follows (mM): NaCl 452; KCl 9·8; $CaCl_2$ 10·6; $MgCl_2$ 48; Tris 10 (buffered at pH 8·0 with HCl). D-tubocurarine (1 to 5×10^{-5} M) or eserine (5×10^{-7}–10^{-6} M) was added to the perfusing fluid when necessary. During the experiment, bathing fluid was continuously circulated with a peristaltic pump. Temperature of the bath was kept about 11° C by a cooling unit.

Staining of acetylcholinesterase. Karnovsky's acetylthiocholine method was used (Karnovsky & Roots, 1964). The embryos were fixed in 10 % formalin containing 1 % $CaCl_2$ for 3 min at room temperature. Then they were washed in distilled water and incubated in the acetylthiocholine-containing medium for 1·5 hr at 20° C. The embryos were then washed with distilled water again and were dehydrated by a gradual series of ethyl alcohol (65, 70, 80, 90, 99 %). Benzene was added to make embryos transparent. Control experiments were performed by incubating embryos in the medium without substrates. In order to examine pseudocholinesterase, embryos were incubated in medium containing butyrylthiocholine iodide as a substrate.

RESULTS

Neuromuscular transmission in the striated muscle of the tunicate larva

Excitatory junctional potentials in the muscle cell of the tadpole larva. The tadpole larva of the tunicate is free-swimming during 20–30 hr after its hatching until metamorphosis of the tail portion has finished. During the swimming movement, six rows of striated muscle cells in the tail show repeated single twitches and also show rhythmic contraction for several seconds. When a micro-electrode penetrated intracellularly into a muscle cell, the initial resting potential was usually in the range from -30 to -50 mV, and in successful cases the membrane gradually hyperpolarized to a steady level of -70 mV within a few minutes after the penetration (Text-fig. 2*A*). On this hyperpolarized level of resting membrane potential, we could observe three kinds of activity (Text-fig. 2*A*). The first was sporadic minute depolarizing potentials of 0·2–0·5 mV (Text-fig. 2*A*, *B*, inset). The second was relatively large depolarizing potentials of 5–15 mV or single spikes. The third was grouped discharges with an interval of about 2 min between successive bursts. The second and third

types of activity corresponded to twitches and sustained rhythmic contractions, respectively. Since the critical membrane potential of the spike potentials in this muscle cell is known to be about −30 mV (Takahashi *et al.* 1971), most of the sporadic depolarization should be excitatory junctional potentials (e.j.p.s) of neuromuscular transmission.

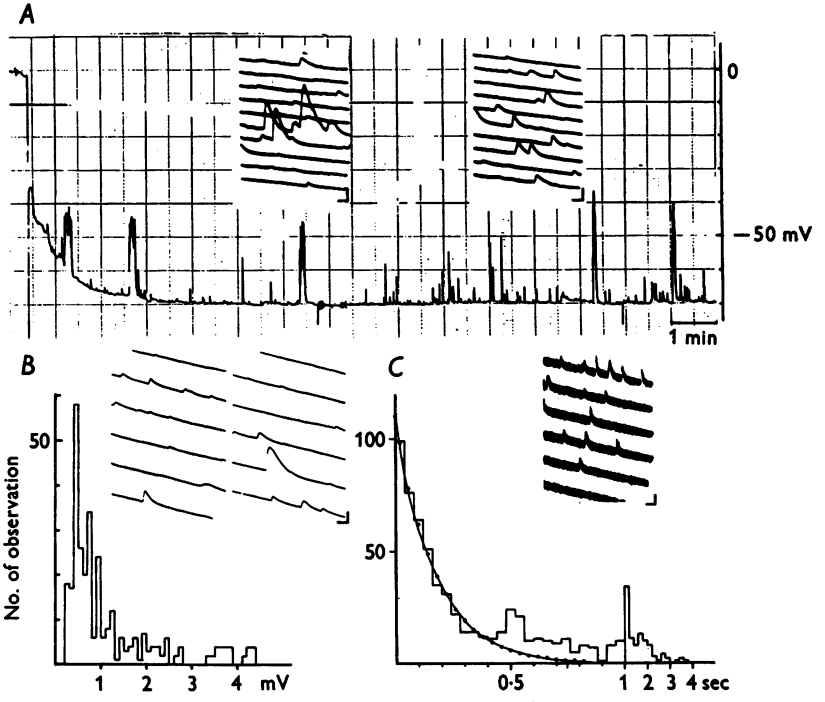

Text-fig. 2. *A*, membrane potential and e.j.p.s. on DC pen recorder. The time of touching the electrode to the surface of the embryo and injecting a transient current was indicated by the initial abrupt potential change. The insets illustrate the continuous records of e.j.p.s on moving film with faster time base (calibration 5 mV, 50 msec). *B*, amplitude–frequency distribution of miniature e.j.p.s of a hatched larva. The inset shows the occurrence of miniature e.j.p.s for which this histogram was obtained (calibration 2·5 mV, 50 msec). *C*, distribution of the time interval between successive e.j.c.s. The shortest interval which could be resolved in this experiment was 5 msec. The observed intervals were grouped in bins of 40 msec. The curve was drawn from the equation $n = N\Delta t/T \exp(-t/T)$ to fit the distribution for the short intervals, $\Delta t = 40$ msec, $T = 176$ msec. The inset shows the occurrence of the e.j.c.s, for which the histogram was obtained (calibration 1 nA, 50 msec).

Since the morphology and pattern of innervation of this tunicate neuromuscular junction are little known, the term 'excitatory junctional potentials (e.j.p.s)' was used in the present experiments instead of 'end-plate potentials (e.p.p.s)' which is used to refer to vertebrate neuromuscular junctions.

It is impossible to stimulate the motor nerve separately and analyse the elementary properties of e.j.p.s because the nerve cells in the tunicate larva are small in size, and the branching pattern and mode of innervation of motor nerves are not known in *Halocynthia roretzi*. However, as shown in Text-fig. 2*B*, inset, the sporadic depolarizing potentials showed a fairly uniform time course in spite of various peak amplitudes. Further, the interval histogram of successive e.j.p.s was distributed exponentially (Text-fig. 2*C*). The curve in Text-fig. 2*C* is drawn from the equation $n = N\Delta t/T \exp(-t/T)$ expected for the waiting time of a Poisson process (Fatt & Katz, 1952), where T is the mean interval, N is the total number of observations and n is the number of events between t and $t+\Delta t$. There was a deviation above the value predicted by this equation in the interval range larger than 0·5 sec. This may be due to contamination of the events that occurred at intervals of 0·5 and 1 sec such as twitches or sustained rhythmic contractions. It is reasonable to consider the minute sporadic depolarizations as miniature e.j.p.s induced by spontaneous quantum release from the nerve terminals, by analogy to other vertebrate neuromuscular junctions, and to analyse the elementary properties of the e.j.p.s.

As shown in Text-fig. 2*A*, *B*, inset, the e.j.p. rose to its peak rapidly and decayed slowly and approximately exponentially. The peak time was 20–30 msec and the half-decay time was 50–100 msec. There was a tendency for a large e.j.p. to have a large half-decay time. Since the I–V relation of the embryonic muscle cell membrane in the tunicate is known to be non-linear and marked anomalous rectification exists around −70 mV (Takahashi *et al.* 1971), a large half-decay time may be due to an apparent large membrane time constant with larger depolarization. Peak amplitudes of the e.j.p.s ranged from 0·5 to 5 mV and a sample of the histogram of the amplitudes is illustrated in Text-fig. 2*B*. In the histogram the largest peak is around 0·5 mV and the distribution is skewed to the right. The peak at 0·5 mV probably corresponds to that of a unitary miniature e.j.p. in this neuromuscular junction. The second or the third peak may indicate the release of two or three quanta at the same time and the large e.j.p. of more than 5 mV may be a grouped release by synchronized action potentials at the motor nerve terminals. These results suggest that quantal release exists also in the neuromuscular junction of the tadpole larva.

Reversal potential of excitatory junctional potential. Since the steady-state I–V relation in the embryonic muscle membrane of the tunicate was markedly non-linear, the amplitude of e.j.p.s was not linearly related to the membrane potential. In order to avoid this difficulty and to find the reversal potential of the e.j.p., excitatory junctional currents (e.j.c.s) were

measured under the voltage clamp condition (Text-fig. 2*C*, inset) and their potential dependency was observed. Text-fig. 3*A* shows e.j.c.s at four levels of holding membrane potential. Within the potential range

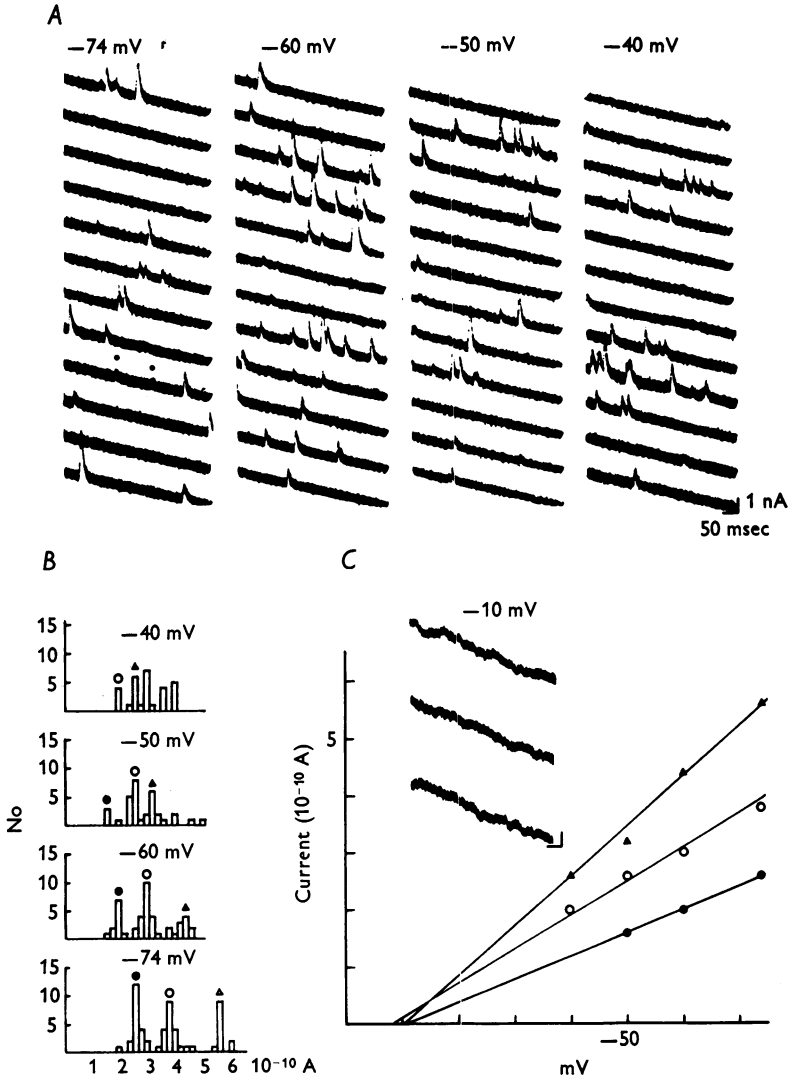

Text-fig. 3. Relationship between the amplitude of e.j.c.s and the membrane potential. *A*, e.j.c.s of the hatched larva at four different holding potentials. *B*, amplitude–frequency histogram of e.j.c.s at four levels of membrane potential shown in *A*. *C*, the estimated amplitude of the current at the peak of the histogram (filled circle, open circle and triangle) was plotted against the membrane potential (further explanation, see text). The inset illustrates the e.j.c.s at a holding potential of −10 mV (calibration 1 nA, 50 msec).

from −74 to −40 mV, the time courses of e.j.c.s were fairly similar and the e.j.c. reached its maximum very rapidly and decayed exponentially (see Text-fig. 4*C*; Takeuchi & Takeuchi, 1959; Kordaš, 1972; Magleby & Stevens, 1972*a*). The rise time to the peak was 0·65 to 2 msec (1·6 ± 0·9 msec, mean and S.D., $n = 30$) and the decay time constant was estimated as 6–10 msec (8·5 ± 1·8 msec, mean and S.D., $n = 22$) at −60 mV, 11° C. In toad striated muscle, two types of miniature end-plate currents (e.p.c.s) are observed, which usually differ only in rising phase but not in falling phase; normal miniature e.p.c.s which have rise times of 50–300 μsec and slow miniature e.p.c.s which have rise times of 0·5–5 msec (Gage & McBurney, 1975). The value of this tunicate miniature e.j.c.s was similar to that of the slow miniature e.p.c.s of the toad. The time constant of the falling phase was the same order as that of the toad miniature e.p.c.s at the same membrane potential and temperature. The Q_{10} of the falling phase was about 2, but the Q_{10} of the rise time could not be estimated accurately because of wide scatter in measurement (Table 2). It seemed less than 1·3.

The above result suggests that the onset and decay of the current may be governed by different processes as in the case of other vertebrate neuromuscular junctions. The initial phase seems to be governed by a process with low activation energy, possibly diffusion, and the falling phase by a process with high activation energy, possibly a conformational change in membrane protein (Magleby & Stevens, 1972*b*).

Fig. 3*B* shows amplitude histograms of e.j.c.s at four levels of the membrane potential as illustrated in Text-fig. 3*A*. The amplitudes were not uniformly distributed but were clustered around certain preferred values, as most clearly shown in the histogram at −74 mV. The peaks were found at current levels of 2·6, 3·9, and $5{\cdot}3 \times 10^{-10}$ A in the histogram of −74 mV. It was assumed that there should be one more peak around $1{\cdot}3 \times 10^{-10}$ A level but the smallest e.j.c.s (indicated by dots in Text-fig. 3*A* could not be accurately measured due to the presence of large noise currents. Thus it could be considered that the e.j.c. due to the release of one quantum was $1{\cdot}3 \times 10^{-10}$ A at −74 mV from the difference of the current levels between successive peaks in the histogram. As the holding potential shifted in the positive direction, the corresponding peaks in the histogram seemed to shift to smaller values of current, and the intervals between successive peaks were reduced. At −40 mV it was assumed that two peaks were concealed in the background noise of about $1{\cdot}5 \times 10^{-10}$ A. The estimated current levels at the corresponding peaks were plotted against the membrane potentials in Text-fig. 3*C*. Three straight lines obtained corresponded to three peaks respectively and all lines intersected the abscissa at the same level of about −10 mV. Similar experiments

TABLE 2. Excitatory junctional currents in the tunicate larva. The reversal potential of miniature e.j.c.s in the hatched larva

Embryo no.	Temp. (°C)	Holding potentials (mV)	Amplitudes of e.j.c. at −70 mV P_1	P_2	P_3*	Reversal potentials P_1	P_2	P_3 (mV)	Remarks†
H 73	10	−70, −60, −49·5, −33	2 15	3 2	.	−10	−9	.	
H 81	11	−70, −60, −50, −40	2·0	3·55	.	−10	−12	.	
H 83	20	−74, −60, −50, −40	2·45‡	3·7‡	5·25‡	−9	−9·5	−12·5	Temperature
H 92	11	−70, −60, −50, −40	2·5	3·7	5·0	−10	−12	−12·5	Eserine
H 93	12	−70, −60, −50, −40	.	3·0	4·5	.	−10	−11·5	Eserine
Mean and S.D.						−10·4 ± 1·3 (n = 12)			

* $P_1P_2P_3$: peaks of the amplitude-frequency histogram of miniature e.j.c.s in 10^{-10} A.
† Effect of eserine or temperature (11–25° C) was examined on the time course of miniature e.j.c.s.
‡ Corrected for the values at −70 mV.

Appearance of giant or medium sized e.j.c.s

Embryo no.	Temp. (°C)	Stage hour	Giant e.j.c.s	Medium sized e.j.c.s	Hatched type e.j.c.s	Remarks
BH109	11	54	+ + +	+	.	Current clamp
BH111	11	54	+ + +	+	.	Current clamp
BH121	11	54	+ +	+ +	.	Voltage clamp
BH148	11·5	54–55	+ + +	+ + +	.	Current clamp*
BH156	11	54	+ +	+ +	.	Current clamp
BH161	11	54	+ +	+ +	.	Current clamp
BH160	11	55	+ +	+ +	.	Current/voltage clamp
BH162	11·5	55–56	+	+ + +	+	Current/voltage clamp*
BH123	10·5	56	−	+ +	+	Current clamp
BH163	11	56	−	+	+ + +	Current/voltage clamp

* Effect of DTC upon the giant e.j.p.s was examined.

were successfully performed in five embryos (Table 2). The mean value and standard deviation of the reversal potential were $-10{\cdot}4 \pm 1{\cdot}3$ mV ($n = 12$). The observation that the reversal potential was about -10 mV was consistent with the observation that when the membrane potential was held at -10 mV, no detectable current flow was observed except for noise as shown in Text-fig. 3*C*, inset. These results indicate that the e.j.c.

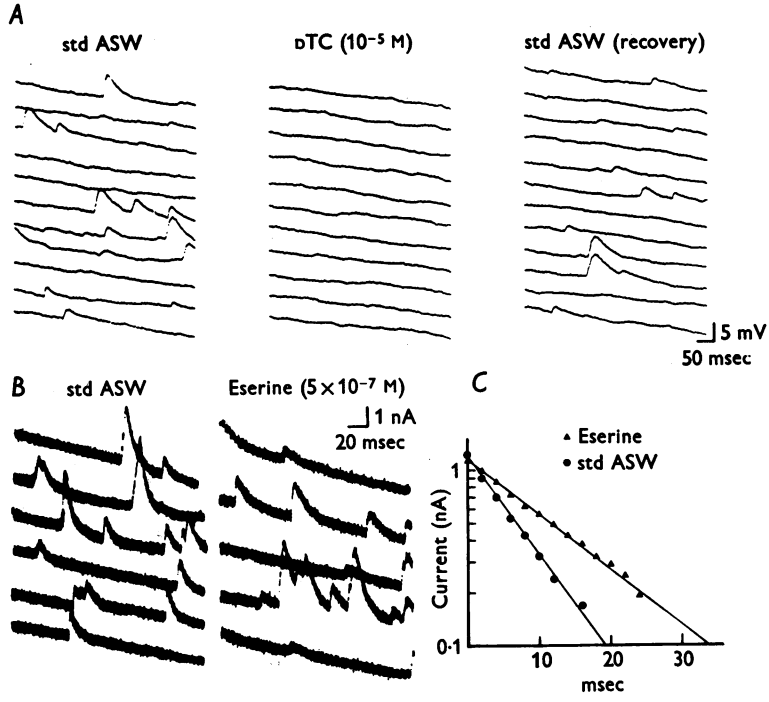

Text-fig. 4. *A*, effect of D-tubocurarine (10^{-5} M) on e.j.p.s. *B*, effects of eserine (5×10^{-7} M) on e.j.c.s. The membrane potential was held at -70 mV. *C*, semilogarithmic plots of the falling phases of e.j.c.s against time.

induced by the release of one quantum is linearly related to the driving force, $E_m - E_r$ (E_m, membrane potential; E_r, reversal potential), and the supposed correspondence of the peaks among the different potential levels is correct. Thus, it was concluded that the e.j.c. in this tunicate larva is also described by the equation $I_{e.j.c.} = g_{e.j.c.}\ (E_m - E_r)$ as in the case of frog striated muscle (Takeuchi & Takeuchi, 1960).

Effects of D-tubocurarine (D-TC) and eserine. Neuromuscular transmission at vertebrate end-plates so far investigated is cholinergic. Since the tunicate, which belonges to the protochordates, is closely related to the vertebrate, it is probable that the neuromuscular transmitter is ACh. The effects of DTC and eserine on these e.j.p.s or e.j.c.s were therefore

examined. On application of 10^{-5} M-DTC in std ASW, e.j.p.s were completely suppressed within 10 min (Text-fig. 4*A*). The e.j.p.s which had disappeared recovered usually within 30 min after the removal of DTC from the ASW (Text-fig. 4*A* recovery).

Anticholinesterases are well known to prolong the falling phase of the cholinergic end-plate current in the vertebrate (Takeuchi & Takeuchi, 1959; Kordaš, 1972; Magleby & Stevens, 1972*a*; Katz & Miledi, 1973; Magleby & Terrar, 1975) and miniature e.p.c.s (Gage & McBurney, 1975). Text-fig. 5*B* illustrates the e.j.c.s in std ASW and after the application of 5×10^{-7} M eserine in std ASW (Table 2). When the dose of eserine was more than 10^{-6} M, the e.j.c.s began to be suppressed as previously reported in the vertebrate end-plates (Eccles & MacFarlane, 1949; Fatt, 1954). The holding membrane potential was -70 mV throughout the experiment. In Text-fig. 4*C*, the falling phases of e.j.c.s with and without eserine in std ASW were plotted on a logarithmic scale against the time after the peaks of e.j.c.s. Since both falling phases described straight lines, it was clear that the e.j.c. had an exponential decay either with or without eserine. The time constants of the falling phases were 7 and 13·5 msec with and without eserine respectively. Thus, eserine prolonged the falling phase just as in the case of the e.p.c.s of the frog.

ACh potential. From the effects of DTC and eserine upon the e.j.c.s it was suggested that the transmitter is ACh. Responses of the larval muscle membrane to iontophoretically applied ACh were examined by observing currents under voltage clamp conditions. In the hatched tadpole larva the responses to ACh were significantly dependent upon the location of the ACh-injecting micropipette. It seemed that there were many sensitive spots distributed over the whole muscle surface and each sensitive spot showed a different sensitivity to ACh (Text-fig. 5*C*). It was found that the sensitive spots around the muscle region at the middle of the tail had the lowest threshold for ACh (Text-fig. 5*C*). Text-fig. 5*A* shows responses to four different amounts of ACh injected through a micropipette at the most sensitive spot. The duration of an injecting pulse was fixed at 0·5 msec and the ACh amount was altered by changing the current intensity. The time course of the ACh response was not significantly dependent upon the amount of ACh. This suggested that the ACh pipette was positioned close to the sensitive spot and the receptors were not saturated by ACh (Feltz & Mallart, 1971*a*). The response current reached a peak 90 msec after the onset of the pulse and decayed approximately exponentially. The peak time and half decay time were 132 ± 65 msec ($n = 7$, Table 3) and 139 ± 65 msec ($n = 7$) respectively. The peak ACh currents were plotted against nanocoulombs (nC) used for applying ACh in Text-fig. 5*B*. The dose–response curve was a linear relation between

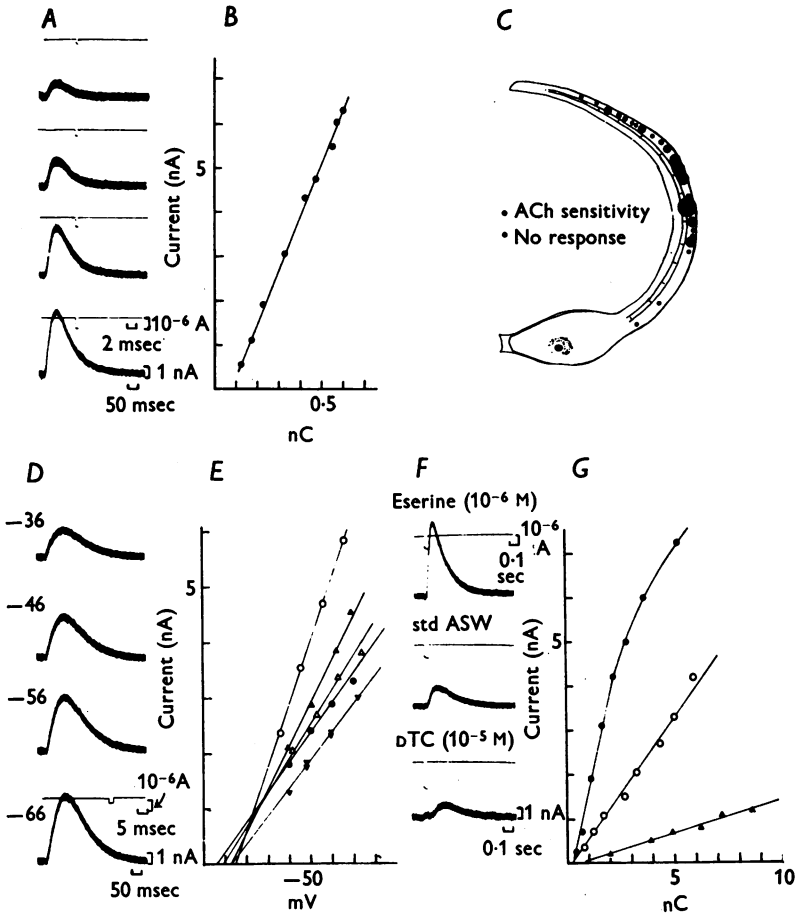

Text-fig. 5. Response of the larval muscle membrane to iontophoretically applied ACh under voltage clamp conditions. *A*, dose–response of ACh current at −70 mV membrane potential (lower and thick trace). The duration of the injecting pulse was fixed and the ACh amount was altered by changing the current intensity (upper and thin trace, note different sweep speed). *B*, the peak of ACh current against nCs used for applying ACh; dose–response curve. *C*, relative ACh sensitivity over the surface of the muscle membrane. ACh sensitivity (mV/nC) was represented by the size of the filled circles. Open circles indicate points on the muscle membrane which had no detectable response to applied ACh. *D*, ACh current responses to the same injecting pulse at four different levels of membrane potentials. The pulse duration was 2·5 msec and 9·5 nC was injected. The numbers at left indicate the membrane potentials. *E*, the peak currents were plotted against membrane potentials. Different symbols indicate different embryos. Open circles were obtained from the embryo shown in *D*. *F*, the effects of DTC and eserine on ACh current. DTC (10^{-5} M) or eserine (10^{-6} M) was added in std ASW. *G*, dose–response curve in eserine (filled circle) and in DTC (triangle). Open circle, control in std ASW. Possibility of the movement of the ACh pipette during the experiment was ruled out by observing the same dose–response curve before and after application of eserine or DTC.

TABLE 3. The response of the muscle membrane to iontophoretically applied ACh in the tunicate embryo before (BH) and after (H) hatch

Embryo no.	Stage (hr)	Temp. (°C)	Holding potential (mV)	Peak time (msec)	ACh sensitivity nA/nC	ACh sensitivity 10^{-2} mV/nC*	ACh sensitivity Bath†	Reversal potential (mV)	Remarks‡
H87		11	−74	200	0·21				
H88		11	−74	220	0·12				
H90		11	−70	100	15·1			−9·5	Eserine
H91	Hatched	12	−40	180	0·16			−14·0	Eserine, DTC
H92		11	−70	70	18·8			−8·5	Eserine
H93		12	−72	60	25			−11·5	Eserine
H94		12	−70	100	12·6			−14·0	
Mean and S.D.				132 ± 65 (n = 7)	10·3 ± 10·2 (n = 7)			−11·5 ± 2·5 (n = 5)	
BH56	22	9				0			
BH60	23	10				0			
BH127	33	10·5				0			
BH102	37	11				0			
BH95	38	11				0			
BH99–101, 128, 132–133, 149, 164 (total eight embryos, 38 hr stage, temp. 11–12° C)						0			
BH96	39	6					+		
BH103	39	11					+		
BH105	39	11·5					+		
BH104	39	11	−70	750		0·17			
BH137	39	12·5	−55	1000		4·6			
BH139	39	11·5	−51	1500		11			
BH140	39	11	−48	750		0·53			
BH116	39	11	−58	600	0·005			−15·5	

TABLE 3 (*cont.*)

Embryo no.	Stage (hr)	Temp. (°C)	Holding potential (mV)	Peak time (msec)	ACh sensitivity nA/nC 10^{-2} mV/nC*	Bath†	Reversal potential (mV)	Remarks‡
BH114	40	11	−60	400	0·003			
BH130	41	11·5	−67·5	300	0·03		−12·5	Eserine
BH98	42	11	−60	340	0·18		−12	
BH115	42	11	−60	240	0·03		−7·5	Eserine, DTC
BH106	43	11	−68	380	0·01		−10, −12	
BH107	43	11	−57	340	0·025			
BH141	44	11	−53	200	0·15			
BH143	44	11	−60	220	0·12		−15	Eserine
BH144	44	11	−49	380	0·07			
BH148	44	11	−58	350	0·04		−11, −12·5	
BH119	50	11	−68	200	0·03		−15	
BH117	52	11	−50	380	0·06		−9, −10	
BH122	54	10	−50	150	0·08		−13	
BH110	64	11	−70	260	0·08		−10	
Mean and S.D.				§ 295 ± 82 (n = 14)			−11·8 ± 2·4 (n = 14)	

* ACh response was observed by the membrane potential change.
† ACh was applied in the ASW perfusing in the bath.
‡ Effects of eserine and/or DTC upon ACh current were examined.
§ The data obtained from stage 40 to 64 were averaged.

ACh current and nC of applied ACh as in case of other cholinergic end-plates (Harrington, 1973; Kuffler & Yoshikami, 1975). The sensitivity to ACh could be defined by the slope of the dose–response curve, the value being 12·6 nA/nC in this case. The sensitivity of each spot in the hatched tadpole larva ranged from 0·1 to 25 nA/nC (mean 10·3 nA/nC, $n = 7$, Table 3).

Text-fig. 5*D* shows ACh currents with the same injecting pulse at four different membrane potentials. The pulse duration was 2·5 msec and 9·5 nC was injected in total. The peak ACh current was $5{\cdot}8 \times 10^{-9}$ A at a membrane potential of -66 mV. With increased depolarization, the peak current decreased successively to 4·7, 3·55, and $2{\cdot}35 \times 10^{-9}$ A at potential levels of -56, -46 and -36 mV respectively. The peak currents of this case (open circle) and those recorded from other embryos were plotted against the membrane potentials in Text-fig. 5*E*. There was a straight line on which the ACh current was linearly related to the membrane potential; if the conductance changes were assumed to be independent of membrane potential, the line could be extrapolated, crossing the abscissa at about -10 mV ($-11{\cdot}5 \pm 2{\cdot}5$ mV, $n = 5$, Table 3). Since the estimated reversal potential of the ACh current was very close to that of the e.j.c., it supported the view that the transmitter at the larval neuromuscular junction in the tunicate is ACh.

Effects of eserine and DTC upon the ACh current are illustrated in Text-fig. 5*F*. The middle trace in Text-fig. 5*F* was a control in std ASW and the upper trace was an ACh current with 10^{-6} M eserine in the ASW. The current rose more rapidly and the peak current was three times larger than that of the control. The ACh current was markedly reduced by adding 10^{-5} M-DTC to the ASW (lowest trace in Text-fig. 5*F*). The effects of eserine and DTC on the dose–response curve are illustrated in Text-fig. 5*G*. The sensitivities to ACh were 0·7, 2·2 and 0·1 nA/nC in std ASW, in the ASW with eserine, and in the ASW with DTC respectively. Thus in the ASW with 10^{-5} M-DTC the sensitivity was reduced by more than 5 times. The above results suggest that the ACh response in the tunicate larva is similar to the response of the vertebrate end-plate.

Development of cholinergic transmission in the larval muscle of the tunicate

Since it was found that neuromuscular transmission in the tunicate larva is mediated by ACh, it seemed desirable to determine the activity of AChE, the appearance of ACh receptors, and the generation of miniature e.j.p. during the development of the embryonic muscle cells.

Acetylcholinesterase. In the tunicate *Ciona intestinalis* it has been reported that AChE appears as early as the neurula stage and it is confined to the presumptive muscle cells (Durante, 1956; Whittaker, 1973). How-

ever, the exact time relation of its appearance to the development of ACh receptors has not been determined. Therefore, the AChE activity was re-examined histochemically by Karnovsky's method in the embryo of *Halocynthia roretzi*. Pl. 2 illustrates the location of AChE in the embryos at four different stages. The esterase activity became visible histochemically as early as the 27 hr stage when the blastopore had been closed and the neural plate began to invaginate. As described later, the stage was just 12 hr before the appearance of ACh receptors. At the time of appearance, AChE was already localized only in the presumptive muscle regions, which have been described by Conklin (1905*a*, *b*) and are situated bilaterally and caudally in the embryo. The developmental stage when the esterase activity began to be detected seemed identical with that described in the case of *Ciona intestinalis*. AChE activity remained localized exclusively on the muscle cell surface throughout the later development, as illustrated in Pl. 2. It was difficult to determine the degree of AChE activity from the difference in the strength of the staining, although there may be some increase in the activity during development. If the incubation time for the enzyme reaction was more than 30 min at 30° C, the muscle cells were stained more or less diffusely. However, when the incubation time was much shorter than 30 min, the surface of the muscle cells was irregularly stained and showed a tendency for the midportion or the region at one third from the head in the tail to be more heavily stained. This region may correspond to the region of high ACh sensitivity.

The contribution of pseudocholinesterase can be excluded because when butyrylthiocholine instead of acetylthiocholine was used for the substrate in Karnovsky's method, the muscle cells were not stained at all during the same incubation time.

Development of ACh receptors. Since the classical study by Conklin and the staining of AChE enable us to identify the location of muscle cells very easily, the development of ACh receptors on the presumptive muscle cell membrane was traced in the whole embryo. In order to decide critically the first appearance of ACh responses in the developmental stages, the application of ACh was started at the late stage of the gastrula or 22 hr stage when AChE was not yet found. At this stage the ACh pipette could approach the surface of the muscle membrane because the presumptive muscle cells were exposed on the surface of the embryo. In later stages the muscle cells were covered with an unicellular layer of epithelium, but both intracellular micro-electrodes and ACh-injecting pipettes were introduced through the intercellular gaps to touch the surface of muscle cells. The ACh response was not evoked before the 39 hr stage, when the tail length became one third of that in the hatched tadpole larva. The 39 hr stage was found to be critical, for no trace of ACh response

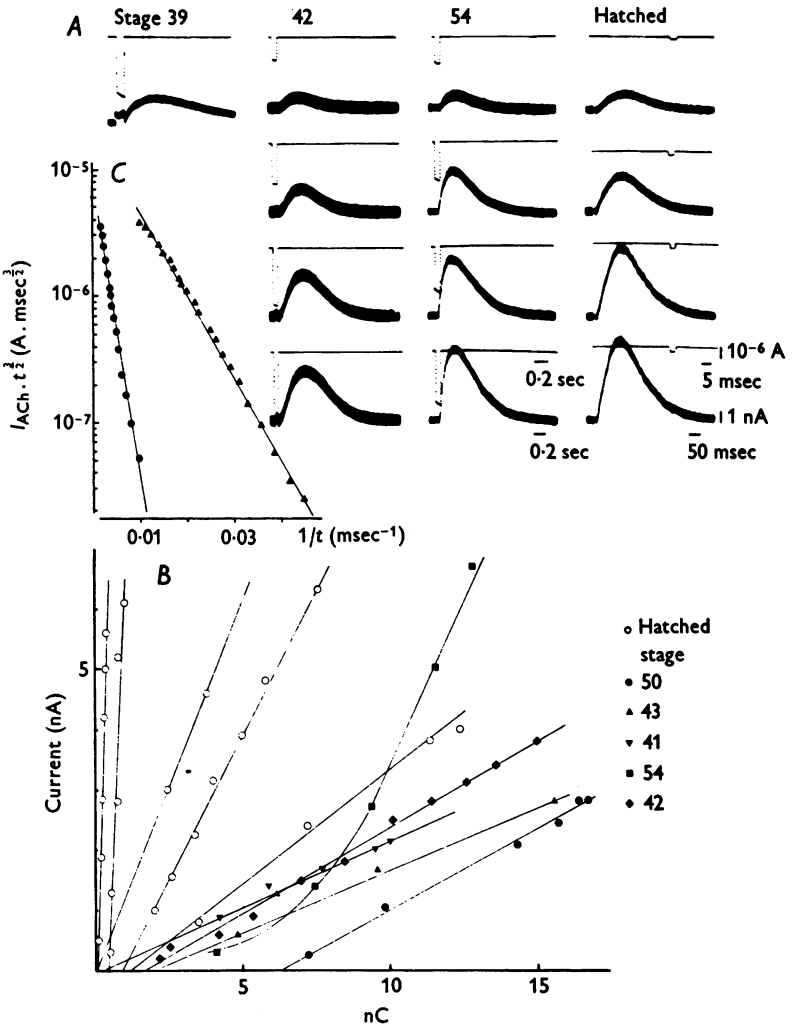

Text-fig. 6. Development of ACh receptors. *A*, ACh currents to various amount of iontophoretically applied ACh at four different stages. Thirty-eight hours was a critical stage because no trace of ACh response could be evoked before this time. *B*, dose–response curves at various stages of development. When the holding membrane potential was different, the curve was corrected to -70 mV by using the equation $I_{ACh} = g_{ACh}\ (E_m - E_r)$ and by assuming that the reversal potential E_r was -10 mV. *C*, Semi-logarithmic plot of $I_{ACh}.t^{3/2}$ against $1/t$ (see text). Circles indicate ACh current at the 41 hr stage, peak time 400 msec. Triangles, from hatched larva, peak time 90 msec.

could be evoked before 38 hr in any region of the muscle cell membrane. This result was further confirmed by experiments in which 10^{-5}–10^{-4} M-ACh was added to the bathing fluid and the resultant depolarization observed (Table 3).

After the initial appearance of ACh response, the muscle cell membrane seemed to become much more sensitive to ACh within 2 hr. Text-fig. 6*A* illustrates the current responses to iontophoretically applied ACh at four different stages, including the 39 hr stage. At the critical 39 hr stage as large a pulse as 41·5 nC in 100 msec induced only a small and slowly rising response. The peak time of the ACh current was about 600 msec and the half-decay time was more than 500 msec. From 39 to 41 hr ACh responses greatly increased and the peak time was reduced to 200–400 msec, and then they remained relatively unchanged until larval hatching. The average peak time at 40–60 hr stages was 295 ± 82 msec ($n = 14$, Table 3). As shown in Text-fig. 6*A*, there were some variations of both the sensitivity and the peak time during those stages. Since the variations were not consistently associated with the advancement of stages, we considered that they may be due to the difference in distances between the sensitive spots and the tip of ACh pipettes because of the presence of a layer of epithelium. As to the regional difference of ACh sensitivity within an embryo, we always attempted to obtain the optimal position of the ACh pipette on the muscle cell membrane of that embryo as described in the Methods. The slow time course observed at the 39 hr stage seemed not to be due to the separation of the pipette from the muscle surface, but to the low density of ACh receptors and to saturation of the receptors by the large dose of ACh. This view was supported by the observation that lower doses of ACh made the response much smaller but its time course slightly faster (Feltz & Mallart, 1971*a*).

After the larval hatching the ACh response clearly increased and ACh sensitivity, as described later, sometimes exceeded 100 times that usually observed in the embryonic muscle cells. The peak time seemed to be reduced and peak times less than 100 msec were frequently observed as illustrated in Text-fig. 6*A*. The average peak time was 132 ± 65 msec ($n = 7$, Table 3). The reduction of the peak time may be explained by the closer contact of the pipette with the muscle surface because the trypsin treatment in the hatched tadpole larva, described in the Methods, efficiently expanded the intercellular gaps in the epithelium. However, the increase in the amplitude of the current response should be mainly due to an increase in density of ACh receptors in muscle cells.

The ACh response may change in its amplitude and time course as a function of the distance from the tip of ACh pipette to the sensitive spot such as an end-plate (del Castillo & Katz, 1955; Feltz & Mallart, 1971*a*; Dreyer & Peper, 1974). Assuming

that ACh is released instantaneously from a point source and ACh receptors are located at a point with variable distance (r) from the source, ACh concentration at the receptor site, (ACh), will be described by the following equation (Carslaw & Jaeger, 1959; del Castillo & Katz, 1955);

$$(\mathrm{ACh}) = \frac{Q}{8(\pi Dt)^{3/2} \exp(r^2/4Dt)}, \quad (1)$$

where Q is coulombs injected and D is the diffusion constant. If ACh current is linearly related to (ACh) at the receptors, ACh currents multiplied by $t^{3/2}$ will be inversely proportional to the time after the injecting pulse on a semilogarithmic scale. Text-fig. 6*C* illustrates two samples of ACh currents which had different peak times of 400 and 90 msec at the 41 hr stage (●) and hatched larva (▲) respectively. The result indicated that the time course of ACh response in this embryonic muscle was nicely fitted with the prediction from eqn. (1).

The peak time T is proportional to the square of r in accordance with eqn. (1). Therefore, the ratio of the apparent sensitivities with different distances from the source will be as follows:

$$(\mathrm{ACh})_{\mathrm{peak},r_1}/(\mathrm{ACh})_{\mathrm{peak},r_2} = (r_2/r_1)^3 = (T_1/T_2)^{3/2}. \quad (2)$$

Thus, the apparent sensitivity should be inversely proportional to peak time to the 1·5 power if the ACh receptor density were constant.

The increase in the ACh sensitivity after the larval hatching was much greater than that expected from the reduction of the peak time. Thus the higher density of ACh receptors in the hatched larva was considered responsible for this increase instead of the shorter diffusion distance of ACh due to the closer contact of the pipette.

Changes in the reversal potential during development will be another important factor which may have an influence upon the variation of the peak amplitudes of ACh responses. It has been questioned whether the extra-junctional response after denervation shows the same reversal potential as the junctional response, and it is possible that the non-innervated membrane during development can show an ACh response with a different reversal potential (Feltz & Mallart, 1971*a*, *b*; Mallart, Dryer & Peper, 1976). In this tunicate embryo, the reversal potential of ACh currents at various stages was determined. Text-fig. 7*A* shows three ACh currents at 41, 52 and 68 hr stages at four different levels of the membrane potential. In Text-fig. 7*C*, the peak currents were plotted against the membrane potential, different symbols illustrating different stages. The results indicated that the reversal potential was always around -10 mV and there was no systematic alteration during development. The mean value of the reversal potential estimated from the combined data at various developmental stages was $-11{\cdot}8 \pm 2{\cdot}4$ mV ($n = 14$, Table 3).

Recently it has been reported that the relation between ACh current and the membrane potential is non-linear mainly below -70 mV in the frog end-plate (Mallart *et al.* 1976). We observed linear relations in the potential range between -35 and -70 mV and had no evidence that they were still linear beyond that range.

Thus there might be some errors in the estimated reversal potential, although it is unlikely that there are systematic differences in our estimation between the embryonic stages and the hatched larval stage.

The effect of eserine on the ACh current is illustrated in Text-fig. 7*B*. The peak current was slightly increased after application of 5×10^{-7} M eserine in std ASW at the 41 hr stage, but the reversal potential was not changed. The reduced effect of eserine on ACh current may be due to the lower AChE activity at 41 hr.

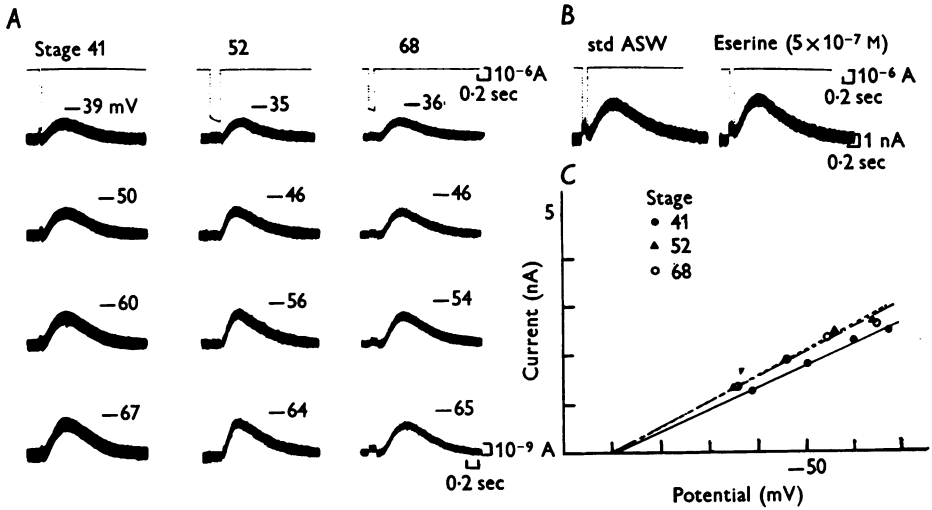

Text-fig. 7. Reversal potentials of ACh responses of developing embryonic muscle membrane. *A*, ACh currents at four different membrane potentials. In each case, the size of injecting ACh pulse was constant. *B*, effect of eserine (5×10^{-7} M) on ACh current at the 41 hr stage. The holding potential was −67 mV. The amount of injecting current pulse was the same in both records. *C*, the peaks of the currents illustrated in *A* were plotted against the holding potentials at stages indicated by the symbols.

In order to compare the sensitivities to ACh among various stages more quantitatively, the dose–response curves were obtained as illustrated in Text-fig. 6*B*. There were some variations in the holding membrane potentials among the embryos examined. Therefore, the amplitudes of ACh currents in Text-fig. 6*B* were corrected to a potential of −70 mV, assuming that the reversal potential was constant (−10 mV) and ACh currents could be described as $I_{ACh} = g_{ACh}(E_m - E_{r\text{-}ACh})$; g_{ACh} is independent of the potential. ACh sensitivity estimated as the slope of the dose–response curve was plotted semilogarithmically against the hours from fertilization or the stage number of the development in Text-fig. 8. This figure clearly shows that ACh sensitivity appeared suddenly at 39 hr and

remained constant until hatching. After hatching of the larva, high sensitivity over 100 times that usually found in the embryonic muscle cells was frequently observed.

Development of synaptic transmission and giant spontaneous e.j.p.s. The first sign of neuromuscular transmission in the tunicate embryonic muscle was not the appearance of miniature e.j.p.s seen in hatched larva,

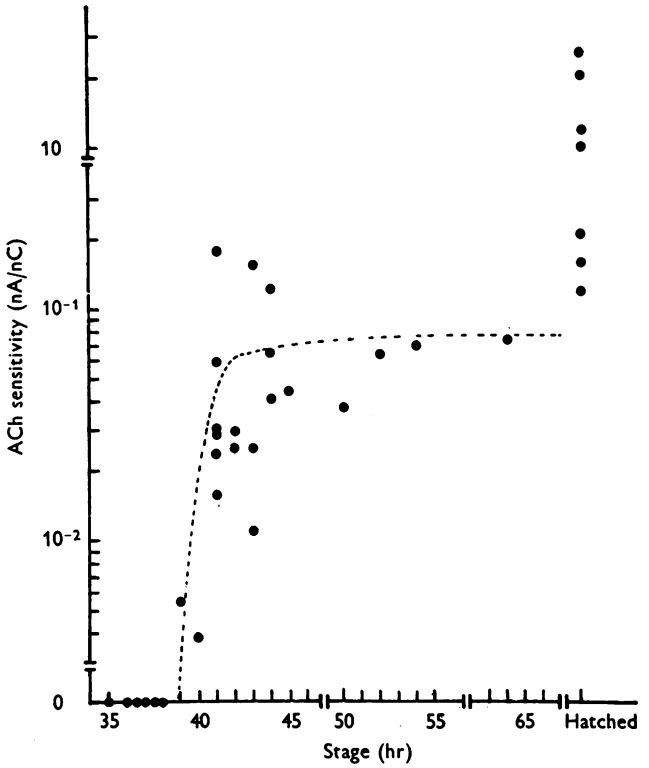

Text-fig. 8. ACh sensitivity (nA/nC) was plotted against the stage hour. The most sensitive spot of the muscle membrane in each embryo was selected for the sensitivity measurement.

but a spontaneous occurrence of two to five grouped giant e.j.p.s which appeared at the 54 hr stage. The current and voltage clamp experiments on these initial e.j.p.s were performed in ten embryos (Table 2). The intervals between grouped giant e.j.p.s were fairly regular as shown in Text-fig. 9*A*, lower record (15–20 sec between e.j.p.s). Therefore, it was reasonable to consider that the giant e.j.p.s probably result from regular neural activities which may occur locally in nerve terminals or may be conducted from higher centres, rather than being induced by the same random mechanism as in the case of miniature e.j.p.s.

The giant e.j.p.s were suppressed with 10^{-5} M-DTC in std ASW as shown in Text-fig. 9*D*, indicating that giant e.j.p.s were also transmitted by ACh. The peak time and half-decay time of the potential were 0·03 and 0·05 sec, respectively. In order to rule out the possibility that the

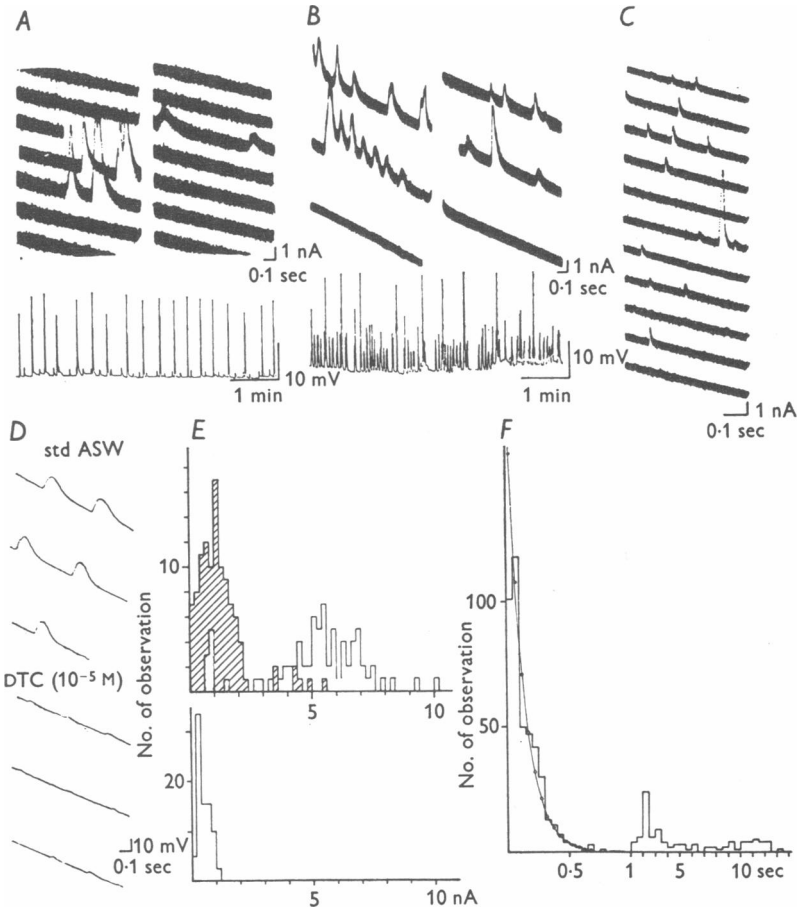

Text-fig. 9. Development of synaptic transmission. *A* and *B*: upper record; giant or medium-sized e.j.c.s under voltage clamp conditions, holding potential −60 mV. Lower record; giant or medium-sized e.j.p.s on DC pen recorder with slow time base. *A*, 54 hr stage. *B*, 55 hr stage, 1 hr after *A*. Note that frequency of medium-sized e.j.p.s has greatly increased in comparison with that of giant e.j.p.s. *C*, miniature e.j.c.s of the hatched larva. Membrane potential, −60 mV. *D*, effect of DTC (10^{-5} M) on giant e.j.p.s. *E*, amplitude-frequency histograms of e.j.c.s. at 54 hr stage (white column), 55 hr stage (dotted column), and the hatched larva (lower histogram). *F*, distribution of time interval of successive medium-sized e.j.c.s in *B*. The curve was drawn from the equation $n = N\Delta t/T \exp(-t/T)$, $\Delta t = 60$ msec, $T = 123$ msec.

slow time course is due to increased effective resistance at these stages as suggested in other developing neuromuscular junctions (Diamond & Miledi, 1962; Bennett & Pettigrew, 1975), the current of the giant e.j.p.s was observed under voltage clamp conditions (Text-fig. 9*A*). The result indicates that the peak time and the time constant of the exponential decay phase were actually prolonged and they were $18{\cdot}0 \pm 4{\cdot}6$ msec ($n = 48$) and $23{\cdot}4 \pm 6{\cdot}9$ msec ($n = 46$, at -60 mV, 11° C) respectively, about 10 times and three times larger than those of miniature e.j.c.s of the hatched larva.

Transition from giant e.j.p.s to miniature e.j.p.s of the hatched larva. The above mentioned giant e.j.p.s were completely replaced by miniature e.j.p.s, which were similar to those of the hatched larva in amplitude and time course within a few hours (Table 2). At the initial step of the transition, medium-sized e.j.p.s of 2–10 mV appeared within 0·5–1 hr. With further advancement of the stages from 54 to 57 hr, both giant and medium-sized e.j.p.s disappeared and were replaced by the usual miniature e.j.p.s (Text-fig. 10*C*). Text-fig. 9*E* shows amplitude–frequency histograms during the transition. In the Figure, e.j.c.s were measured rather than e.j.p.s in order to rule out a possible error due to the change of membrane resistance during these stages. As shown in Text-fig. 9*E*, the distribution of the peak amplitude of e.j.c.s was abruptly changed from the white column (54 hr stage) to the hatched column (55 hr stage). The results indicate that the peak amplitude jumped from $5{\cdot}5 \times 10^{-9}$ A in giant e.j.c.s to 10^{-9} A in medium-sized e.j.c.s. With further development the usual miniature e.j.c.s were observed within a few hours (Text-fig. 9*E*, lower histogram). It should be noted that, although the transition among three types of e.j.c.s was rather discontinuous, there were transitional phases where two types of e.j.c.s coexisted (Text-fig. 9*B*, lower record).

The frequency of the medium-sized e.j.c.s was much higher than that of giant e.j.c.s. The interval histogram for the occurrence of medium-sized e.j.c.s shown in Text-fig. 9*B* was mostly exponentially distributed as expected from a Poisson random process (Text-fig. 9*F*). Although there was some regularity of events at an interval of about 2 sec, which may be due to some rhythmic activity at presynaptic nerve terminal or from central structures, it is reasonable to consider that the medium-sized e.j.p.s. may be induced by a random mechanism similar to that in the hatched larva.

The time course of e.j.c.s became much faster during the process of synaptogenesis. The falling phases of both giant and medium-sized e.j.c.s decayed exponentially as shown in Text-fig. 10*A* (filled circle). The time constants of these decays were $23{\cdot}4 \pm 6{\cdot}9$ ($n = 46$) and $19{\cdot}2 \pm 5{\cdot}3$ msec ($n = 7$) at -60 mV and 11° C, respectively. Subsequently, the

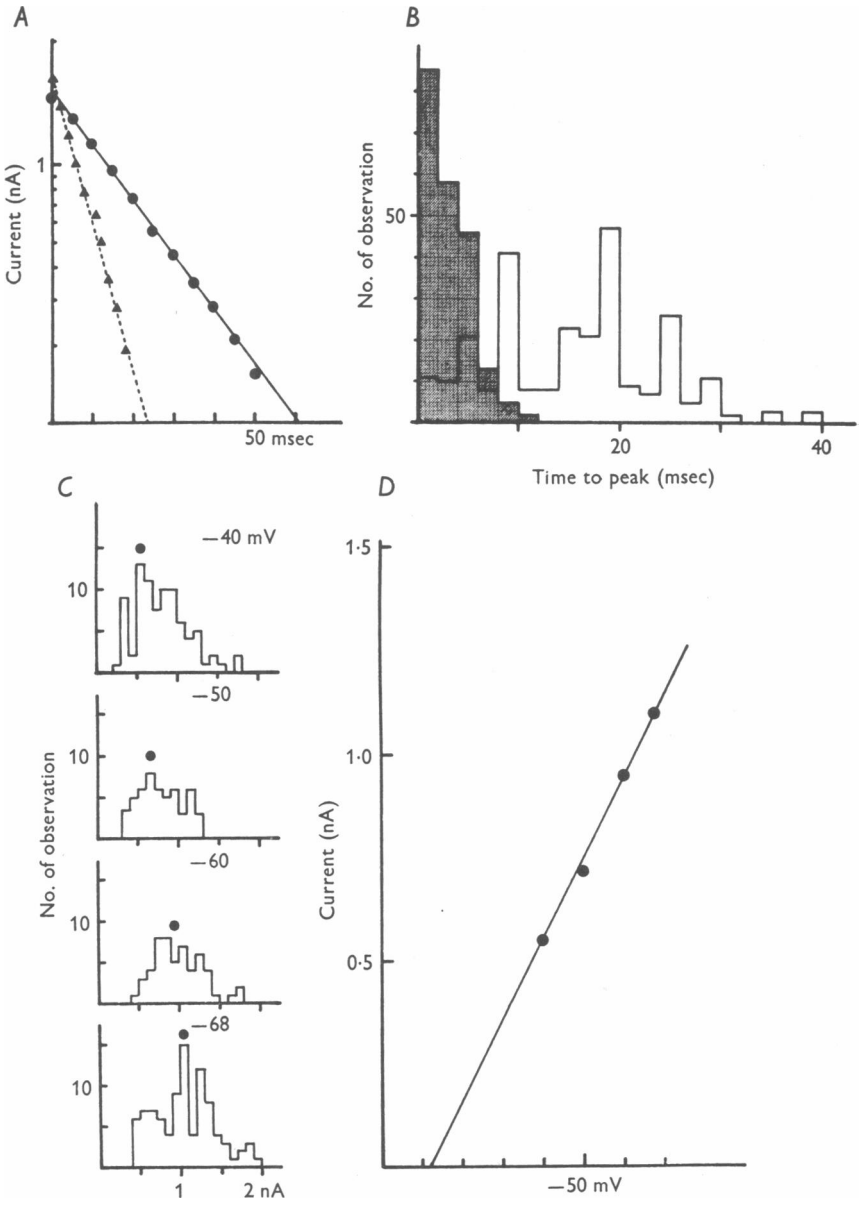

Text-fig. 10. *A*, falling phases of medium-sized e.j.c.s (filled circle) and miniature e.j.c.s of the hatched larva (triangle) were plotted semilogarithmically against time. The time constants are 20·5 and 7·9 msec respectively. *B*, comparison of peak time of giant and medium-sized e.j.c.s (open column) with miniature e.j.c.s of the hatched larva (dotted column). *C*, amplitude–frequency histogram of medium-sized e.j.c.s at four different membrane potentials. *D*, relationship between peak amplitudes of e.j.c.s and membrane potentials. The amplitudes at the peaks of the distributions in *C* (dots) were plotted against membrane potentials.

time constant of the falling phase decreased within a few hours to those of miniature e.j.c.s in hatched larva (time constant of $8{\cdot}5 \pm 1{\cdot}8$ msec, $n = 22$, Text-fig. 10*A* triangle). The rise time of giant and medium-sized e.j.c.s were $18{\cdot}0 \pm 4{\cdot}6$ ($n = 48$) and $16{\cdot}3 \pm 6{\cdot}9$ msec ($n = 49$) respectively (Text-fig. 10*B*, open column). These values also became almost the same as those in hatched larva within a few hours (Text-fig. 10*B*, hatched column).

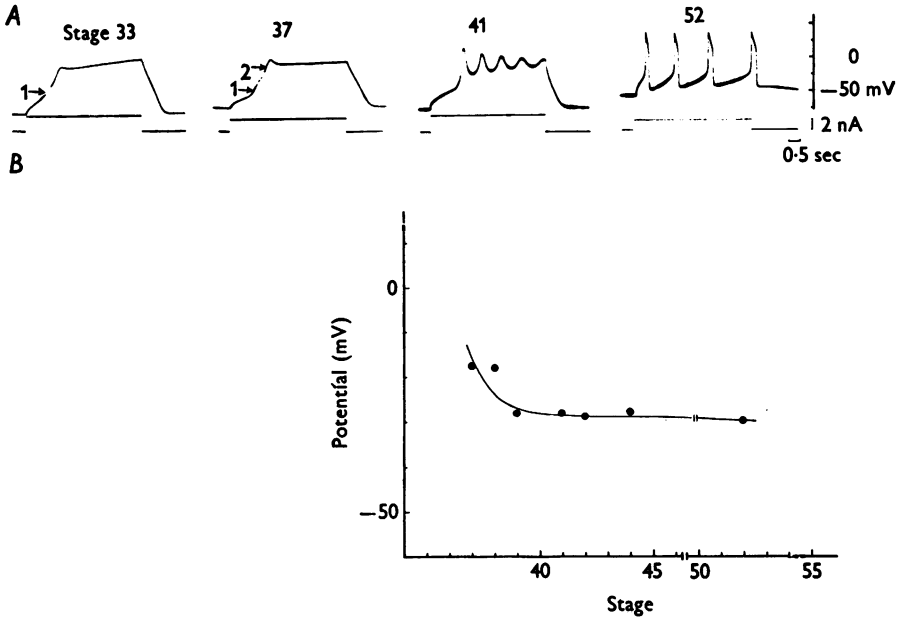

Text-fig. 11. Development of Ca action potentials. *A*, muscle membrane responses to depolarizing constant currents at four different stages. Arrow 1, inflexion due to Na action potential; arrow 2, inflexion due to Ca action potential. *B*, critical membrane potentials for Ca action potential of the muscle membrane at each stage of development were plotted against stage hours.

Text-fig. 10*C* illustrates amplitude histograms of medium-sized e.j.c.s at four levels of membrane potential. The current at the peaks of the histograms was plotted against the membrane potential (Text-fig. 10*D*); the results indicated that the reversal potential of the e.j.c.s was -10 mV, the same as that of miniature e.j.c.s of the hatched tadpole.

Generation of Ca action potential and appearance of ACh sensitivity. As described above, ACh sensitivity appeared in the embryonic muscle membrane at the 39 hr stage. The stages seemed to correspond to the time when Ca action potentials can be first elicited in the muscle cell of

the tunicate larva, as reported previously (Takahashi *et al.* 1971; Miyazaki *et al.* 1972).

Text-fig. 11*A* shows local responses or action potentials elicited by constant current stimulation in the muscle cell membrane at various stages around 39 hr. Before 38 hr the depolarization during constant current stimulation showed two inflexions (1, 2) on the rising phase, one of which at more positive levels of the membrane potential has been confirmed to be due to Ca current (K. Takahashi & M. Yoshii, personal communication). The inflexion at more negative levels of the membrane potential remained after removal of Ca and is considered to be due to Na current. After 40 hr the inflexion by Ca current was displaced to more negative levels of the membrane potential and the maximum rate of rise of Ca action potentials become increased.

In association with the increase in Ca current, the critical membrane potential for Ca current shifted from -20 to -30 mV also at 38–40 hr stages (Text-fig. 11*B*). The critical membrane potential for Ca current in the tunicate egg membrane has been known as -10 mV in std ASW (Okamoto *et al.* 1976). Thus it may be inferred that generation of Ca action potential at 38–40 hr stages is partly due to the lowered threshold for Ca current.

It was concluded in the larval muscle membrane of the tunicate that the initial appearance of ACh receptors occurs exactly at the time when Ca action potential is first observed.

DISCUSSION

Development of acetylcholine receptors. Neuromuscular transmission in the embryonic muscle cells of the tunicate began to function 15 hr after ACh sensitivity appeared, while AChE activity was first demonstrated 12 hr ahead of this time. Although no special attempt was made to prove that there were no inactivated forms of the esterase or receptors, at the present moment we assume that they were just assembled upon the membrane surface when their activities were first demonstrated and that they could be measured by the response to applied ACh. It has been reported that the amount of ACh receptors measured by the binding capacity for α-bungarotoxin is exactly proportional to that estimated by the response to iontophoretically applied ACh (Hartzell & Fambrough, 1972).

It is reported in cultured myotubes without any nervous explants that ACh receptors are present (Fambrough & Rash, 1971; Hartzell & Fambrough, 1973; Fischbach & Cohen, 1973; Vogel, Sytkowski & Nirenberg, 1972). During development ACh sensitivity is known to spread widely over the muscle cell surface and after the innervation is established it is

localized around the end-plate region (Diamond & Miledi, 1962). It is claimed that in cultured myotubes even the localization of the receptors is found ahead of the innervation and the nerve seems to be attracted by the region of high receptor density (Sytkowski *et al.* 1973; Fischbach & Cohen, 1973). Appearance of ACh sensitivity ahead of synapse formation is also demonstrated in the tunicate larva. This suggests that the ACh receptors are essential prerequisite for neuromuscular transmission both *in vitro* and *in vivo*. However, the validity of this suggestion must be considered with some reservation, since the receptor intoxicated by α-bungarotoxin is not known to disturb the normal pattern of reinnervation (Jansen & Van Essen, 1975) nor to suppress the innervation of cultured myotubes (Steinbach, Harris, Patrick, Schubert & Heinemann, 1973). Further studies will be necessary to determine what aspects of ACh receptors are inducers of the neuromuscular junction.

The localized activity of AChE in the embryonic muscle of the vertebrate has been found to be concomitant with the formation of the discrete region of nerve termination (Mumenthaler & Engel, 1961; Terävāinen, 1968; Atsumi, 1971) and no definite experiments have been reported which demonstrate the preliminary presence of the esterase far ahead of the synapse formation. The activity of the enzyme is initially very low around the newly formed synapses in co-cultured myotubes and nerve explants (Robbins & Yonezawa, 1971; Köenig, 1973). Anticholinesterase has almost no effect upon the time course of the end-plate potentials or miniature e.p.p.s in the cultured muscle cell (Fischbach, 1972; Kidokoro & Heinemann, 1974). In the tunicate embryo, the esterase was clearly demonstrated 12 hr before the appearance of ACh receptors and eserine was always effective for potentiating ACh responses. The early existence of the esterase may suggest that AChE has a role of an inducer for cholinergic systems besides its function as a modulator of transmission. The classical studies by Reverberi (1961) shows that small doses of anticholinesterase applied at the gastrula stage of a tunicate suppresses the initiation of the tail movement of the hatched tadpole larva, though the morphological features of the tail seem to be completely normal. Even in the vertebrate end-plates a small amount of the esterase may be present ahead of the synapse formation and exert an inductive influence upon the cholinergic system.

In the tunicate embryo the abrupt development of ACh receptors coincided with the appearance of Ca action potentials and the sudden increase in Ca current. The critical membrane potential of this newly developed Ca action potential was -30 mV and was much more negative than that of the Ca current found in the initial egg membrane, that is -10 mV (Okamoto *et al.* 1976). Therefore the sudden increase in Ca

current may result from the lowered threshold for the current. The critical levels for the current in the voltage sensitive ionic channels have been understood in terms of the surface potential at both outer and inner surfaces of the membrane (Frankenhaeuser & Hodgkin, 1957; Gilbert & Ehrenstein, 1969; H. Ohmori and M. Yoshii, in preparation). Thus it is possible that a general increase in the negative charges on the outer surface of the membrane or a decrease at the inner surface may cause assembly of ACh receptors and a negative shift in the critical membrane potential at the same time. There are several reports suggesting that the negative charges carried by the polysaccharide which are attached to the membrane surface are profoundly influential in cellular differentiation in embryos (Schaeffer, Schaeffer & Brick, 1973; Kosher & Searls, 1973). However, another type of explanation is also worth considering. It is known that a decrease in the intracellular ionized Ca induces Ca action potentials in crustacean striated muscle and increased ionized Ca above 10^{-7} M abolishes Ca current (Hagiwara & Nakajima, 1966). The internal concentration of Ca ions may be regulated by the action of mitochondria (Lehninger, 1970). Almost all mitochondria which were present in the unfertilized egg are segregated in the presumptive muscle cells in the tunicate larva (Reverberi, 1961). The accumulated mitochondria in the muscle cells occupy most of the volume in the cytoplasm since the myofibrils in the larval muscle are very scanty and form only a thin, one micron layer beneath the plasma membrane. The recent study by Hartzell & Fambrough (1973) demonstrates that the assembly of ACh receptors in the membrane is an energy-dependent process, since ATP facilitates the assembly and a decoupling agent, dinitrophenol, suppresses it. Thus, it is also possible that the enhanced activity of mitochondria is directly responsible for the correlation between the generation of electrical excitability and the assembly of ACh receptors.

Giant and medium-sized excitatory junctional potentials. It has been reported that amplitude distributions of miniature e.p.p.s are usually skewed or multi-modal during development (Fischbach, 1972; Kidokoro & Heinemann, 1974; Bennett & Pettigrew, 1975) and during reinnervation (Birks, Katz & Miledi, 1960; Miledi, 1960; Dennis & Miledi, 1974). It was suggested that incomplete packages are responsible for these uncommon distributions (Dennis & Miledi, 1974). Miniature e.p.p.s of extraordinarily large amplitude also have been frequently observed during development (Diamond & Miledi, 1962; Robbins & Yonezawa, 1971; Fischbach, 1972). In the present experiment the giant and medium-sized e.j.p.s appeared only at the beginning of synapse formation. We could observe a transitional phase of a few hours in which these giant and medium-sized e.j.p.s co-existed with miniature e.j.p.s of the type usually

found in hatched larva, and then were totally replaced by miniature e.j.p.s. The intervals between giant e.j.p.s were fairly constant but those between medium-sized e.j.p.s were distributed as expected from a Poisson random process. This suggested that two different types of ACh release were present during the development: a type of giant e.j.p.s which might be evoked by action potentials spontaneously occurring at nerve terminal or rhythmic spike activity from central structures, and a type of medium-sized e.j.p. which has a release mechanism similar to that of miniature e.j.p.s of the hatched larva.

The amplitude–frequency distribution of miniature e.j.p.s in the hatched tadpole larva itself showed the distribution of a rather immature type of synapse since it was also skewed and multi-modal even after the transitional phase. This may suggest that the development of synaptic function is incomplete in the tunicate larva. Since the muscle cells were electrotonically connected to each other and their space constant was relatively long compared with the length of a muscle cell (see Methods), the recorded e.j.c.s may not be derived from only one junction but may consist of those from several junctions which were recorded simultaneously. Thus, the skewed distribution of e.j.c. amplitude may also be due to multiple innervation on the functionally united group of muscle cells (Bennett & Pettigrew, 1975).

The time courses of giant and medium-sized e.j.p.s were quite slow in comparison with that of miniature e.j.p.s. The release of the transmitter may be prolonged at newly formed synapses, and AChE may not be functioning to destroy the extraneous ACh. Also, since there is evidence which suggests that the rising phase of the e.j.c.s is determined by diffusion processes inside of the synaptic clefts, the wide clefts in newly formed synapses and the consequent long distances for diffusion may delay the peak of the e.j.p.s considerably. There is no evidence of delayed release at new synapses. AChE activity in myoneural junctions progressively increases during development (Mumenthaler & Engel, 1961; Terävāinen, 1968; Atsumi, 1971). Thus the slow time course of the falling phase may be partly due to low activity of AChE. However, since the rising phase of e.j.p.s is not influenced by AChE activity (Text-fig. 4; Magleby & Terrar, 1975), the slow time course of the e.j.p.s cannot be solely attributed to low activity of AChE. The width of the newly formed synaptic clefts could be estimated from the peak times of 16 msec for medium-sized e.j.c. and 1·6 msec for the miniature e.j.c. Assuming the width in the hatched tadpole larva as 500 Å, the tenfold increase in the peak time will correspond to a width of 1500 Å (see small type P. 20). This estimation seems consistent with electron microscope observations on the developing neuromuscular junction in the chick which suggests that the synaptic clefts are much

wider initially (2000 Å) and later become progressively narrower in association with the differentiation of the post-synaptic membrane (Hirano, 1967).

The authors wish to express their indebtedness to Dr S. Miyazaki for his kind guidance at the early stages of the experiments, and to Dr K. Takahashi for his valuable advice at all stages of this work. They are also indebted to Professor A. Takeuchi and Dr R. Schor for the criticism of the manuscript. They thank Professor H. Shimazu for his constant encouragement. This work was supported by a grant from the Ministry of Education, Science and Culture, Japan.

REFERENCES

ATSUMI, S. (1971). The histogenesis of motor neurones with special reference to correlation of their endplate formation. I. The development of endplate in the intercostal muscle in the chick embryo. *Acta anat.* **80**, 161–182.

BENNETT, M. R. & PETTIGREW, A. G. (1975). The formation of synapses in amphibian striated muscle during development. *J. Physiol.* **252**, 203–239.

BIRKS, R., KATZ, B. & MILEDI, R. (1960). Physiological and structural changes at the amphibian myoneural junction, in the course of nerve degeneration. *J. Physiol.* **150**, 145–168.

CARSLAW, H. S. & JAEGER, J. C. (1959). *Conduction of Heat in Solids*, 2nd edn. Oxford: Clarendon Press.

CONKLIN, E. G. (1905*a*). The organization and cell-lineage of the ascidian egg. *J. Acad. natn. Sci. Philad.* **13**, 1–119.

CONKLIN, E. G. (1905*b*). Mosaic development in ascidian eggs. *J. exp. Zool.* **2**, 145–223.

DEL CASTILLO, J. & KATZ, B. (1955). On the localization of acetylcholine receptors. *J. Physiol.* **128**, 157–181.

DENNIS, M. J. & MILEDI, R. (1974). Electrically induced release of acetylcholine from denervated Schwann cells. *J. Physiol.* **237**, 431–452.

DIAMOND, J. & MILEDI, R. (1962). A study of foetal and new-born rat muscle fibres. *J. Physiol.* **162**, 393–408.

DREYER, F. & PEPER, K. (1974). The acetylcholine sensitivity in the vicinity of the neuromuscular junction of the frog. *Pflügers Arch. ges. Physiol.* **348**, 273–286.

DURANTE, M. (1956). Cholinesterase in the development of *Ciona intestinalis* (Ascidia). *Experientia* **12**, 307–308.

ECCLES, J. C. & MACFARLANE, W. V. (1949). Actions of anti-cholinesterases on endplate potential of frog muscle. *J. Neurophysiol.* **12**, 59–80.

FAMBROUGH, D. & RASH, J. E. (1971). Development of acetylcholine sensitivity during myogenesis. *Devl Biol.* **26**, 55–68.

FATT, P. (1954). Biophysics of junctional transmission. *Physiol. Rev.* **34**, 674–709.

FATT, P. & KATZ, B. (1952). Spontaneous subthreshold activity at motor nerve endings. *J. Physiol.* **117**, 109–128.

FELTZ, A. & MALLART, A. (1971*a*). An analysis of acetylcholine responses of junctional and extrajunctional receptors of frog muscle fibres. *J. Physiol.* **218**, 85–100.

FELTZ, A. & MALLART, A. (1971*b*). Ionic permeability changes induced by some cholinergic agonists on normal and denervated frog muscles. *J. Physiol.* **218**, 101–116.

FISCHBACH, G. D. (1972). Synapse formation between dissociated nerve and muscle cells in low density cell cultures. *Devl Biol.* **28**, 407–429.

FISCHBACH, G. D. & COHEN, S. A. (1973). The distribution of acetylcholine sensitivity over uninnervated and innervated muscle fibers grown in cell culture. *Devl Biol.* **31**, 147–162.

FRANKENHAEUSER, B. & HODGKIN, A. L. (1957). The action of calcium on the electrical properties of squid axon. *J. Physiol.* **137**, 218–244.

GAGE, P. W. & MCBURNEY, R. N. (1975). Effects of membrane potential, temperature and neostigmine on the conductance change caused by a quantum of acetylcholine at the toad neuromuscular junction. *J. Physiol.* **244**, 385–407.

GILBERT, D. L. & EHRENSTEIN, G. (1969). Effect of divalent cation on potassium conductance of squid axons: Determination of surface charge. *Biophys. J.* **9**, 447–463.

HAGIWARA, S. & NAKAJIMA, S. (1966). Effects of the intracellular Ca ion concentration upon the excitability of the muscle fiber membrane of a barnacle. *J. gen. Physiol.* **49**, 807–818.

HARRINGTON, L. (1973). A linear dose-response curve at the motor endplate. *J. gen. Physiol.* **62**, 58–76.

HARTZELL, H. C. & FAMBROUGH, D. M. (1972). Acetylcholine receptors. Distribution and extrajunctional density in rat diaphragm after denervation correlated with acetylcholine sensitivity. *J. gen. Physiol.* **60**, 248–262.

HARTZELL, H. C. & FAMBROUGH, D. M. (1973). Acetylcholine receptor production and incorporation into membranes of developing muscle fibers. *Devl Biol.* **30**, 153–165.

HIRANO, H. (1967). Ultrastructural study on the morphogenesis of the neuromuscular junction in the skeletal muscle of the chick. *Z. Zellforsch. mikrosk. Anat.* **79**, 198–208.

JANSEN, J. K. S. & VAN ESSEN, D. C. (1975). Reinnervation of rat skeletal muscle in the presence of α-Bungarotoxin. *J. Physiol.* **250**, 651–667.

KARNOVSKY, M. J. & ROOTS, L. (1964). A 'direct-coloring' thiocholine method for cholinesterases. *J. Histochem. Cytochem.* **12**, 219–221.

KATZ, B. & MILEDI, R. (1973). The binding of acetylcholine to receptors and its removal from the synaptic cleft. *J. Physiol.* **231**, 549–574.

KIDOKORO, Y. & HEINEMANN, S. (1974). Synapse formation between clonal muscle cells and rat spinal cord explants. *Nature, Lond.* **252**, 593–594.

KÖENIG, J. (1973). Morphogenesis of motor endplate 'in vivo' and 'in vitro'. *Brain Res.* **62**, 361–365.

KORDAŠ, M. (1972). An attempt at an analysis of the factors determining the time course of the end-plate current. I. The effects of prostigmine and of the ratio of Mg^{2+} to Ca^{2+}. *J. Physiol.* **224**, 317–332.

KOSHER, R. A. & SEARLS, R. L. (1973). Sulfated mucopolysaccharide synthesis during the development of *Rana pipiens*. *Devl Biol.* **32**, 50–68.

KUFFLER, S. W. & YOSHIKAMI, D. (1975). The distribution of acetylcholine sensitivity at the post-synaptic membrane of vertebrate skeletal twitch muscles: Iontophoretic mapping in the micron range. *J. Physiol.* **244**, 703–730.

LEHNINGER, A. L. (1970). Mitochondria and calcium ion transport. *Biochem. J.* **119**, 129–138.

MAGLEBY, K. L. & STEVENS, C. F. (1972*a*). The effect of voltage on the time course of end-plate currents. *J. Physiol.* **223**, 151–171.

MAGLEBY, K. L. & STEVENS, C. F. (1972*b*). A quantitative description of end-plate currents. *J. Physiol.* **223**, 173–197.

MAGLEBY, K. L. & TERRAR, D. A. (1975). Factors affecting the time course of decay of end-plate currents: A possible cooperative action of acetylcholine on receptors at the frog neuromuscular junction. *J. Physiol.* **244**, 467–495.

MALLART, A., DREYER, F. & PEPER, K. (1976). Current-voltage relation and reversal potential at junctional and extrajunctional ACh-receptors of the frog neuromuscular junction. *Pflügers Arch. ges. Physiol.* **362**, 43–47.

MILEDI, R. (1960). Properties of regenerating neuromuscular synapses in the frog. *J. Physiol.* **154**, 190–205.

MIYAZAKI, S., TAKAHASHI, K. & TSUDA, K. (1972). Calcium and sodium contributions to regenerative responses in the embryonic excitable cell membrane. *Science, N.Y.* **176**, 1441–1443.

MIYAZAKI, S., TAKAHASHI, K. & TSUDA, K. (1974). Electrical excitability in the egg cell membrane of the tunicate. *J. Physiol.* **238**, 37–54.

MIYAZAKI, S., TAKAHASHI, K., TSUDA, K. & YOSHII, K. (1974). Analyses of non-linearity observed in the I–V relation of the tunicate embryo. *J. Physiol.* **238**, 55–77.

MUMENTHALER, M. & ENGEL, W. K. (1961). Cytological localization of cholinesterase in developing chick embryo skeletal muscle. *Acta anat.* **47**, 274–299.

NASTUK, W. L. (1953). Membrane potential changes at a single muscle end-plate produced by transitory application of acetylcholine with an electrically controlled microjet. *Fedn Proc.* **12**, 102.

OKAMOTO, H., TAKAHASHI, K. & YOSHII, M. (1976). Membrane currents of the tunicate egg under the voltage clamp condition. *J. Physiol.* **254**, 607–638.

REVERBERI, G. (1961). The embryology of ascidians. *Advance in Morphogenesis*, chap. 1, pp. 55–101.

ROBBINS, N. & YONEZAWA, T. (1971). Physiological studies during formation and development of rat neuromuscular junctions in tissue culture. *J. gen. Physiol.* **58**, 467–481.

SCHAEFFER, B. E., SCHAEFFER, H. E. & BRICK, I. (1973). Cell electrophoresis of amphibian blastula and gastrula cells: The relationship of surface charge and morphogenetic movement. *Devl Biol.* **34**, 66–76.

STEINBACH, J. H., HARRIS, A. J., PATRICK, J., SCHUBERT, D. & HEINEMANN, S. (1973). Nerve muscle interaction in vitro. Role of acetylcholine. *J. gen. Physiol.* **62**, 255–270.

SYTKOWSKI, A. J., VOGEL, Z. & NIRENBERG, M. W. (1973). Development of acetylcholine receptor clusters on cultured muscle cells. *Proc. natn. Acad. Sci. U.S.A.* **70**, 270–274.

TAKAHASHI, K., MIYAZAKI, S. & KIDOKORO, Y. (1971). Development of excitability in embryonic muscle cell membranes in certain tunicates. *Science, N.Y.* **171**, 415–418.

TAKEUCHI, A. & TAKEUCHI, N. (1959). Active phase of frog's end-plate potential. *J. Neurophysiol.* **22**, 395–411.

TAKEUCHI, A. & TAKEUCHI, N. (1960). On the permeability of end-plate membrane during the action of the transmitter. *J. Physiol.* **154**, 52–67.

TERÄVÄINEN, H. (1968). Carboxylic esterases in developing myoneural junctions of rat striated muscle. *Histochémie* **12**, 307–315.

VOGEL, Z., SYTKOWSKI, A. J. & NIRENBERG, M. W. (1972). Acetylcholine receptors of muscle grown in vitro. *Proc. natn. Acad. Sci. U.S.A.* **69**, 3180–3184.

WHITTAKER, J. R. (1973). Segregation during ascidian embryogenesis of egg cytoplasmic information for tissue-specific enzyme development. *Proc. natn. Acad. Sci. U.S.A.* **70**, 2096–2100.

EXPLANATION OF PLATES

PLATE 1

Morphological features of the developing embryo. The stages were represented by the time (hr) after fertilization. *A*, gastrula stage (22 hr). *B*, 26 hr stage. *C*, 33 hr stage. *D*, 39 hr stage. *E*, 42 hr stage. *F*, 54 hr stage. *G*, hatched larva. Scale, 100 μm, in *F* for *A* to *F* and in *G* for *G* only. Further explanation, see text. *H*, cross-section of the tail of the hatched larva. *ch*, the notochord; *m*, muscle cells; *epith*, epithelium; *v. end*, ventral endodermal structure; *n*, neural tube.

PLATE 2

Acetylcholinesterase activity of embryos at four different stages of development. Incubation, 1·5 hr at 20° C. The esterase activity became visible histochemically as early as the 27 hr stage and was localized in presumptive muscle cells throughout the development (hatched area).

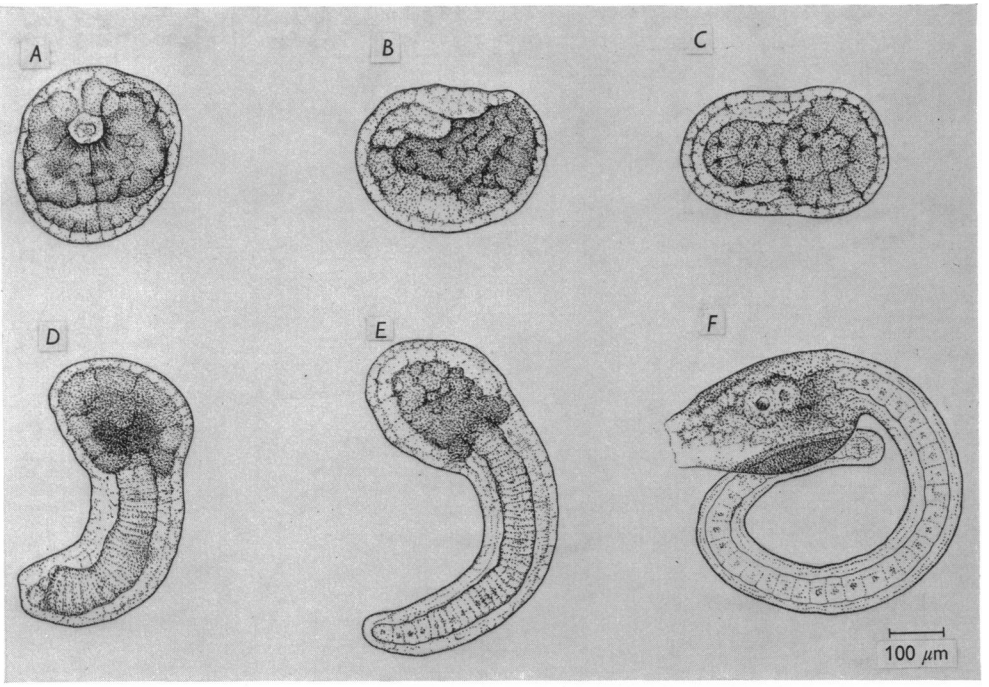
A
B
C
D
E
F
100 μm

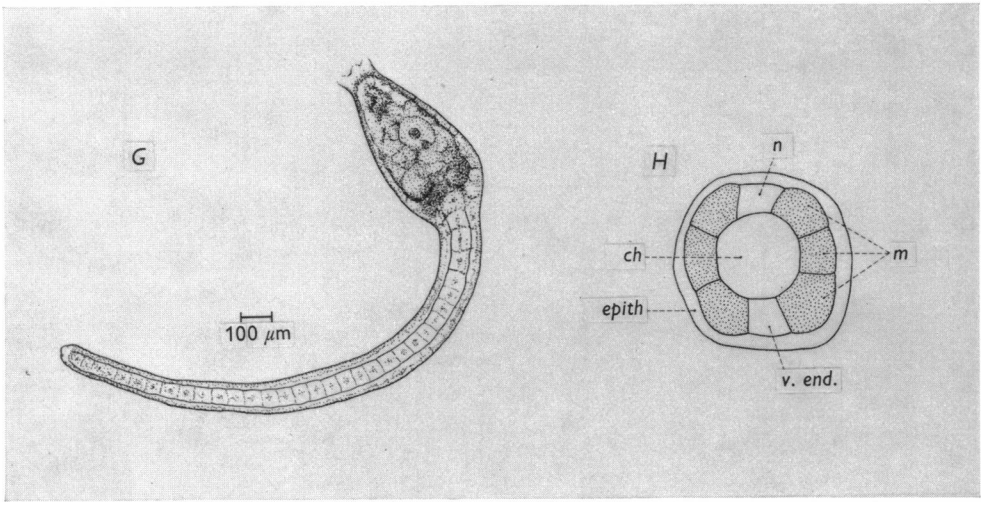
G
100 μm
H
n
ch
m
epith
v. end.

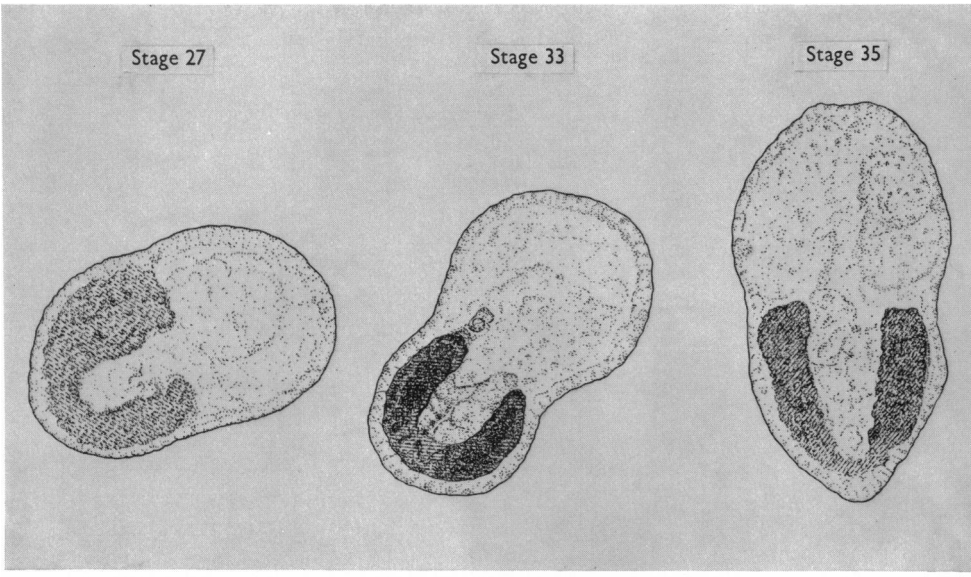
Stage 27
Stage 33
Stage 35